Polymer photonic microstructures for quantum applications and sensing

S. Knauer,[1,2] F. Ortiz Huerta,[2] M. López-García,[2] and J. G. Rarity[2]

[1]Bristol Centre for Nanoscience and Quantum Information, University of Bristol, Tyndall Avenue
Bristol BS8 1FD, UK, Email: sebastian.knauer@bristol.ac.uk
[2]Department of Electrical and Electronic Engineering, University of Bristol, Merchant Venturers Building
Woodland Road, Bristol BS8 1UB, UK

Abstract—**In this paper we present modeling results for efficient coupling of nanodiamonds containing single color centres to polymer structures on distributed Bragg reflectors. We explain how hemispherical and super-spherical structures confine light in small numerical apertures, emitted by such deterministically addressed color centres. Coupling efficiencies of up to 68% within a numerical aperture of 0.34 are found. Moreover, we show how Purcell factors up to 6.2 in structured waveguides are achieved.**

I. INTRODUCTION

Color centers in nanodiamonds are widely used single photon sources, with applications including quantum information processing [1], [2], thermometry [3], magnetometry [4], and fluorescence bio-markers [5]. To increase both the coupling efficiency between nitrogen-vacancy (NV) center's in nanodiamond, and speed of spin read-out, photonic structures are required.

In order to address some of these challenges we present two types of structures on a distributed Bragg reflector [Fig. 1]. The first are hemispherical and super-spherical structures which allow enhanced collection efficiencies and the second structured waveguides that increase the emission rate of a color center.
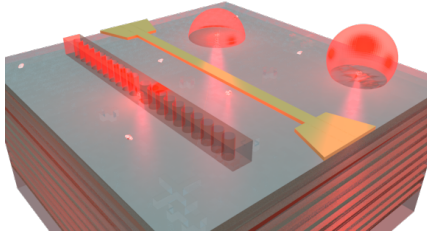

Fig. 1. Concept of nitrogen-vacancy centers in nanodiamonds addressed to photonic structures, e.g. microstructured waveguides, spheres and super-spheres, on a DBR reflector. Displayed is also a deposited microtrack for microwave coherent spin manipulation of the NV's electron and nuclear spin.

II. MODELING OF POLYMER STRUCTURES

A. Hemispheres and super-spheres

Hemispheres, or so-called solid immersion lenses, are widely studied and used, e.g. [6]. Light can be more efficiently coupled and collected, for example to or from a solid state emitter like a NV center. A bigger challenge in the fabrication process are super-spheres, also called Weiserstraß spheres. Some free-standing examples out of glass [7], gallium phosphide [8],

silicon [9] or gallium arsenide [10] have been demonstrated. Here we discuss the difference between substrates based on SiO_2/Ta_2O_5 distributed Bragg reflectors (DBR) and for comparison SiO_2 cover slips. First, we focus on the results of the hemisphere. The optimization is performed for different radii ranging from about 1 μm to 10 μm. An example for the optimal coupling out of these hemisphere (radius 4.16 μm) on top of the DBR is shown with the electric field magnitude in Fig. 2 (top, left). The high reflectivity of the DBR at normal incidence is clearly seen contrasting with light leakage at high incidence angles. The advantage of the DBR in the directional guidance of the light is also shown in the far field projections Fig. 2 (top, right). For the DBR substrate most of the light is confined within a half angle of $15°$, relating to a numerical aperture of approximately 0.5, but part of the light is emitted up to a numerical aperture of about 0.76. For collection efficiency we observe $\approx 65\%$ of the emitted light leaves through the top of the hemisphere while $\approx 35\%$ leaks through the DBR substrate. These values are measured at the central wavelength of 637 nm (zero-phonon-line NV^- center). It is observed that
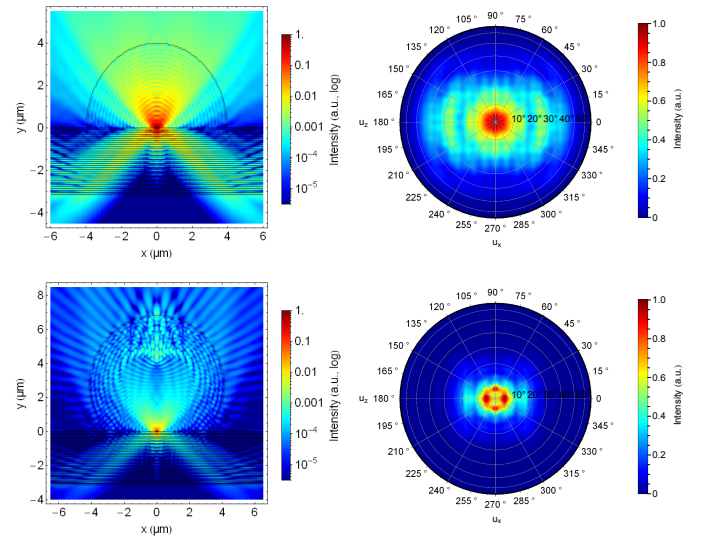

Fig. 2. Left: Electric field magnitude of a polymer hemisphere (top row) and super-sphere (bottom row) with radius 4.16 μm on a SiO_2/Ta_2O_5 DBR. Right: Corresponding far field. The fields are calculated at 637 nm.

the coupling through the top reduces with different radii, due to the amount of light that can constructively interfere with the back reflected light from the hemisphere surface. For the hemisphere with the cover glass substrate (not shown) the radiated light emitted through the top is ≈ 63 %, and through the bottom, i.e. into the cover glass substrate, is ≈ 38 %. This shows that the radiated power through the top interfaces only increases marginally when the DBR substrate is compared with the cover glass although although emitted light is confined to a smaller numerical aperture for the DBR.

The super-sphere with a radius of 4.16 µm is compared to the hemisphere. The electric field magnitude of this super-sphere is shown in Fig. 2 (bottom, left) and the far field projection in Fig. 2 (bottom, right) for the SiO_2/Ta_2O_5 DBR substrate. We observe that the light is more strongly confined in a smaller half angle of approximately $8°$, which relates to a numerical aperture of approximately 0.14, for the DBR substrate. Considering all light emitted, that increases to a maximum numerical aperture of 0.34. Even for the cover glass substrate (not shown) most of the light is confined within a numerical aperture of approximately 0.5. The transmission trough the entire top is approximately 68.5 % and 31.5 % into the DBR substrate. These values are similar to the one presented for the hemisphere on the DBR substrate. Although the losses into the DBR substrate are reduced, a bigger difference between the super-sphere and the hemisphere is found for the cover glass substrate. In the case of the super-sphere on the cover glass approximately 54.2 % is emitted through the entire top and approximately 44.9 % into the cover glass substrate. The losses into the substrate are over 10 % higher than for the DBR substrate as well as 7.5 % higher compared to the hemisphere on the cover glass.

B. Structured waveguides

Current methods rely on a non-deterministic addressing of single nanodiamonds suspended in the polymer of photonic structures. Often cavity distances in nanobeam structures are too small for the coupling to solid states emitters. We present modeling results for the coupling of NV^- centers in nanodiamonds to microstructured waveguides (model in Fig. 3). These NV centers remain near the surface of the substrate, allowing the optical addressing of them and direct writing of the microstructured waveguides over them. We overcome the losses into the substrate by using the SiO_2/Ta_2O_5 DBR utilized in the previous section. Fig. 4 shows an example of the intensity profile of a confined cavity mode within the optimised polymer structured waveguide. The optimization includes the modeling
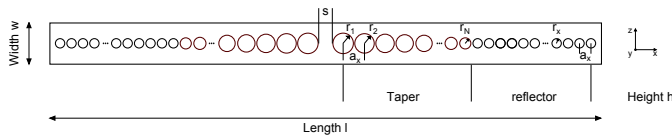
Fig. 3. Waveguide structure with reflectors. The structure consists of a tapered and a reflector region. For more details see text.
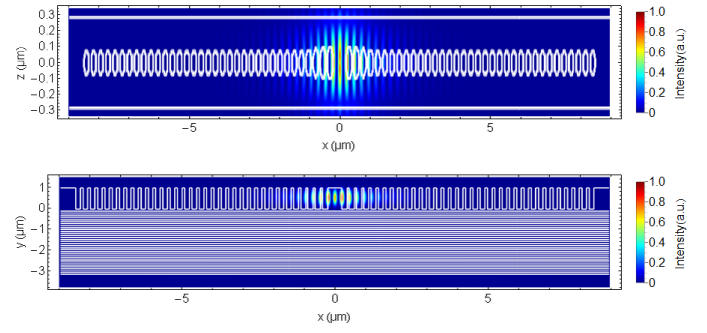
Fig. 4. Intensity profile across the structured waveguide in the x/z-plane (top) and x/y-plane (bottom) for the waveguide mode. Only a small percentage enters the distributed Bragg reflector.

of a taper near the cavity and cavity distance aiming a realistic fabrication with current technology. These structures exhibit Purcell factors up to 6.2.

III. Conclusion

In our work we have modeled how low refractive index polymer structures can be deterministically coupled to single nitrogen-vacancy centers. With hemispheres and super-spheres we achieve strong confinement within small numerical apertures with high collection efficiencies. The confinement may even allow a more precise measurement of the nitrogen-vacancy centers polarization orientation. Moreover, we have shown optimized structured waveguides with Purcell factors up to 6.2.

Acknowledgment

References

[1] R. Hanson and D. D. Awschalom, "Coherent Manipulation of Single Spins in Semiconductors," *Nature*, 453(7198):1043–1049, 2008.
[2] P. C. Maurer et al., "Room-Temperature Quantum Bit Memory Exceeding One Second," *Science*, 336(6086):1283–1286, 2012.
[3] P. Neumann et al., "High-Precision Nanoscale Temperature Sensing Using Single Defects in Diamond," *Nano Lett.*, 13(6):2738–2742, 2013.
[4] J. M. Taylor et al., "High-Sensitivity Diamond Magnetometer with Nanoscale Resolution," *Nat. Phys.*, 4(10):810-816, 2008.
[5] G. Balasubramanian, A. Lazariev, S.R. Arumugam, and De-W. Duan, "Nitrogen-Vacancy Color Center in Diamond-Emerging Nanoscale Applications in Bioimaging and Biosensing," *Curr. Opin. Chem. Biol.*, 20:69–77, 2014.
[6] J. P. Hadden et al., "Strongly Enhanced Photon Collection from Diamond Defect Centres Under Micro-Fabricated Integrated Solid Immersion Lenses," *Appl. Phys. Lett.*, 97(241901):1–3, 2010.
[7] K. Karrai, X. Lorenz, and L. Novotny, "Enhanced Reflectivity Contrast in Confocal Solid Immersion Lens Microscopy," *Appl. Phys. Lett.*, 77(21):3459–3461, 2000.
[8] Q. Wu, G. D. Feke, R. D. Grober, and L. P. Ghislain, "Realization of Numerical Aperture 2.0 Using a Gallium Phosphide Solid Immersion Lens," *Appl. Phys. Lett.*, 75(26):4064–4066, 1999.
[9] W. L. Barnes, "Fluorescence Near Interfaces: The Role of Photonic Mode Density," *J. Mod. Opt.*, 45(4):661–699, 1998.
[10] Z. Liu, B. B. Goldberg, S. B. Ippolito, A. N. Vamivakas, M. S. Ünlü, and R. Mirin, "High Resolution, High Collection Efficiency in Numerical Aperture Increasing Lens Microscopy of Individual Quantum Dots," *Appl. Phys. Lett.*, 87 (7):071905, 2005.